

Lateral torsional buckling behaviour of welded lean duplex stainless steel I section beams

M. Fortan

*Department of Civil Engineering, University of Leuven, Belgium
PhD Fellowship of the Research Foundation Flanders*

O. Zhao & B. Rossi

Department of Civil Engineering, University of Leuven, Belgium

ABSTRACT: Recent studies show that the current lateral torsional buckling design rules in EN 1993-1-1 for carbon steel are very conservative for stocky sections in the medium slenderness range. This phenomenon is also noticeable for stainless steel beams, even though a rather limited amount of experimental results exist. The discrepancy between the tests and the theoretical results is nevertheless reduced if the recently developed lateral torsional buckling formula (Taras & Greiner 2010) is used. This paper investigates the lateral torsional buckling behaviour of welded lean duplex stainless steel I section beams using the finite element (FE) method. On the basis of the experiments and FE models, the accuracy of EN 1993-1-4 and of Taras & Greiner (2010) are assessed. Finally, conclusions on the lateral torsional buckling behaviour of welded lean duplex stainless steel I sections are drawn.

1 INTRODUCTION

Duplex stainless steel types, presenting a microstructure made of austenite and ferrite, share the properties of both families, and are mechanically stronger than either ferritic or austenitic types. More specifically, the stainless steel grades EN 1.4162 and EN 1.4062, also known as lean duplex, which are included in the latest amendment of EN 1993-1-4, are characterized by low nickel content of 1.5% compared to >3% in standard duplex stainless steels, which results in significant reduction in cost compared to other austenitic and duplex grade equivalents. Duplex grades are also characterized by good weldability and can be welded by the same processes used for other grades. This is why recent years have seen an increase in the use of lean duplexes in welded structures (Baddoo 2008) as a good alternative for austenitic or carbon steel equivalents. A number of similarities exist between stainless steel and typical carbon steel but there exist sufficient differences to necessitate specific treatment in design standards for stainless steel, focused on structural applications. The main benefit of stainless steel is the high ductility and strain hardening. However, due to the elastic, perfectly plastic material model, on which EN 1993-1-1 is based, stainless steel cannot be used to its full potential.

In the past decades a lot of research for structural application has been done on stainless steel with alternative design methods that profit of the nonlinear stress-strain behaviour of stainless steels, for example the continuous strength method (CSM) (Theofanous & Gardner 2010). However, the use of this method is not yet allowed according to EN 1993-1-4.

In recent years a lot of work has been done towards, for example, proper classification limits and the instability phenomenon shear buckling (Saliba et al. 2013). However, research and in particular experiments on lateral torsional buckling of stainless steel plate girders remain very scarce.

On top of this, research on the stability of carbon steel beams show that the current rules are too conservative, especially for stocky sections, and a new formulation is proposed (Taras & Greiner 2010). An assessment of the current design rules for stainless steel and this new formulation on the basis of the scarce experiments in literature and numerical simulations is needed. In this paper makes this assessment for beams of the lean duplex grades EN 1.4062 and EN 1.4162, which have the same mechanical properties according to EN 1993-1-4. Various cross-sections and lengths are used to cover the whole range of slenderness for stocky and slender sections.

2 DESIGN RULES

2.1 EN 1993-1-4

The design rules for lateral torsional buckling of stainless steel sections are similar to the ones for carbon steel. The resistance $M_{b,Rd}$ is calculated by multiplying the moment resistance with the reduction factor χ_{LT} . This factor depends on the slenderness λ_{LT} , the imperfection factor α_{LT} and the artificial plateau length λ_0 , equations 1-4. The numerical values can be found in Table 1 for welded I section beams.

$$\lambda_{LT} = \sqrt{\frac{W_y f_y}{M_{cr}}} \quad (1)$$

$$\phi_{LT} = 0.5 \left[1 + \alpha_{LT} (\bar{\lambda}_{LT} - \lambda_0) + \bar{\lambda}_{LT}^2 \right] \quad (2)$$

$$\chi_{LT} = \frac{1}{\phi_{LT} + \sqrt{\phi_{LT}^2 - \bar{\lambda}_{LT}^2}} \leq 1.0 \quad (3)$$

$$M_{b,Rd} = \chi_{LT} \frac{W_y f_y}{\gamma_{M1}} \quad (4)$$

where W_y is the section modulus taking into account the cross-section classification, M_{cr} is the elastic critical moment for lateral torsional buckling and f_y is the yield stress where the 0.2% proof stress is taken for stainless steel because of the non-linear stress-strain behaviour.

2.2 Taras & Greiner (2010)

This study concentrated on the lateral torsional buckling behaviour of compact (class 1-2) and semi-compact (class 3) sections. Only the basic case of lateral torsional buckling, i.e. with a pure bending moment and fork end conditions was considered. However, recent studies investigated non-uniform bending moments (Taras 2010) and a simply supported beam, a cantilever or a two-span beam with a distributed or a single concentrated load (Ebel & Knobloch 2015).

For the basic case, equations 5-8 can be used. They are close to the well-known equations 1-4, however the small differences make up for the conservatism towards stocky sections. The first difference is the use of the plastic moment resistance, even for class 3 sections. Therefore the elastic moment capacity of these cross-sections has to be checked separately. The second and main difference is the inclusion of λ_z and the square root of the strong and weak axis moment resistance in equation 6. The approach however stays the same.

$$\lambda_{LT} = \sqrt{\frac{W_{pl,y} f_y}{M_{cr}}} \quad (5)$$

$$\phi_{LT} = 0.5 \left[1 + \alpha_{LT} (\bar{\lambda}_z - \lambda_0) \sqrt{\frac{W_{y,el} \bar{\lambda}_{LT}^2}{W_{z,el} \bar{\lambda}_z^2}} + \bar{\lambda}_{LT}^2 \right] \quad (6)$$

$$\chi_{LT} = \frac{1}{\phi_{LT} + \sqrt{\phi_{LT}^2 - \bar{\lambda}_{LT}^2}} \leq 1.0 \quad (7)$$

$$M_{b,Rd} = \chi_{LT} \frac{W_{pl,y} f_y}{\gamma_{M1}} \quad (8)$$

Where λ_z is the normalized slenderness for weak axis flexural buckling of the compression flange. For welded cross-sections the imperfection factor α_{LT} is 0.21. However this imperfection factor cannot be compared to the ones of EN 1993-1-1 and EN 1993-1-4 because of the other factors in that term.

Table 1. Numerical values of the imperfection factor and the plateau length for different design methods.

| | EN 1993-1-4 | EN 1993-1-1 | Taras & Greiner (2010) |
|---------------|-----------------|--------------------------------|------------------------|
| | Stainless steel | Carbon steel | Carbon steel |
| α_{LT} | 0.76 | h/b ≤ 2: 0.49 h/b > 2: 0.76 | (0.21) |
| λ_0 | 0.4 | 0.2 | 0.2 |

3 STAINLESS STEEL EXPERIMENTS

3.1 State of the art

Experiments on stainless steel I beams that concern lateral torsional buckling are scarce. However, the few existing results are presented in this paragraph.

The first experiments on lateral torsional buckling of stainless steel beams were performed by Van Wyk et al. (1990). Two cold-formed channel section were spot welded back to back to manufacture the tested I-beams with a width of 30 mm, a height of 50 mm, a thickness of the flanges of 1.2 mm and therefore a web thickness of 2.4 mm. Eight different lengths were tested for each of the three grades: austenitic 304 (EN 1.4301), ferritic 430 (EN 1.4016) and ferritic 3Cr12 (EN 1.4003). The EN 1993-1-4 design rules with both imperfection factors, 0.76 and 0.49, and the design rules of Taras & Greiner (2010) all fail to accurately describe the behaviour of the experiments, Figure 1. The high residual stresses due to cold-forming could have an influence on the buckling behaviour. However it can be concluded that these tests are not representative for the buckling behaviour of welded stainless steel plate girders.

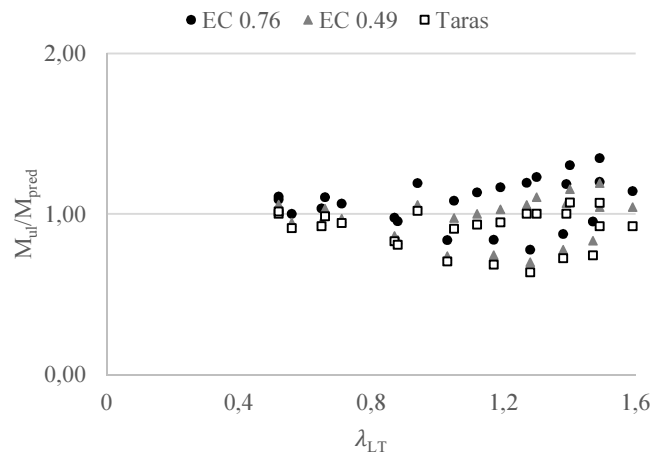


Figure 1. Comparison of Van Wyk et al. (1990) with design rules.

In the context of the further development of EN 1993-1-4, a European research project Burgan et al. (2000) studied, among other things, the flexural behaviour of stainless steel open sections. In the frame of this research, 12 specimens were tested whereof 9 specimens in the austenitic grade EN 1.4301 and 3 specimens in the duplex grade EN 1.4462. It can be seen in Figure 2 that for high slenderness's both the use of imperfection factor 0.49 or the use of the formulation of Taras & Greiner (2010) give better results than the current design rules.

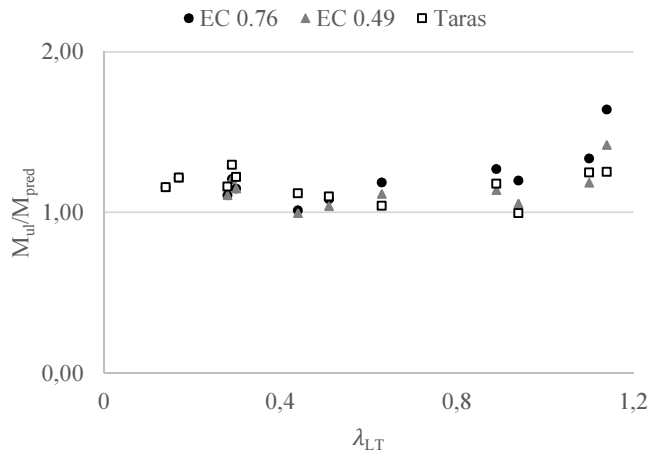


Figure 2. Comparison of Burgan et al. (2000) with design rules.

Recently an experimental study (Wang et al. 2014) and related numerical study (Yang et al. 2014) have conducted an experimental program consisting of 10 beams in the austenitic grade EN 1.4401. As can be seen in Figure 3, the eurocode design rules with imperfection factor 0.49 give the best results. However the new formulation gives similar and for some specimens even slightly worse predictions.

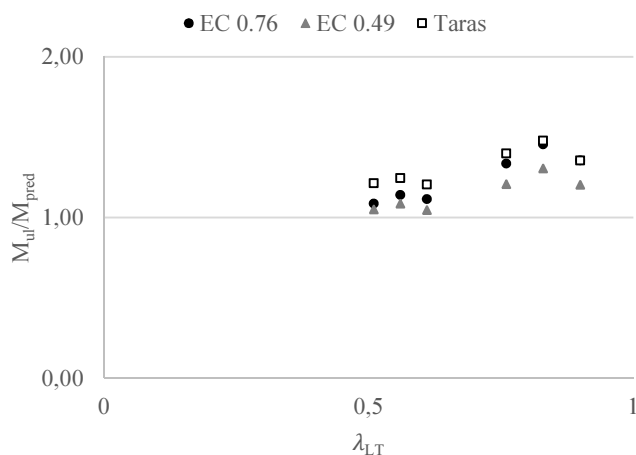


Figure 3. Comparison of Wang et al. (2014) with design rules.

Finally, Hassanein & Silvestre (2013) conducted a numerical research on the flexural behaviour of slender unstiffened plate girders in the lean duplex grade EN 1.4162. The findings of this study confirm the conservativeness of the current design rules as well as the imperfection factor 0.49 giving better results without being unsafe. Because of the slender webs,

the sections are classified as class 4 and hence a comparison using the formulation of Taras & Greiner (2010) is not yet possible.

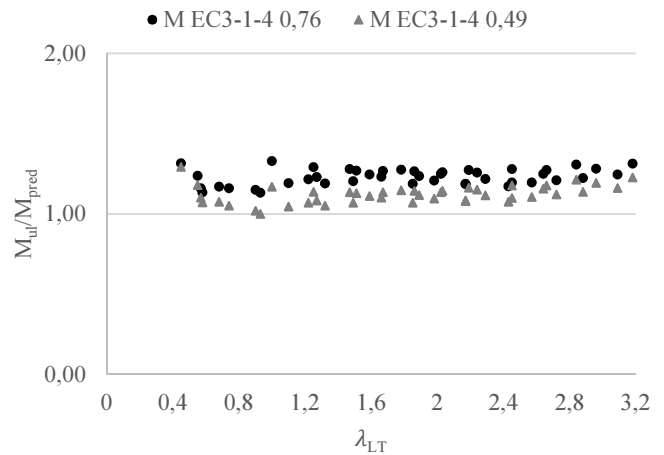


Figure 4. Comparison of Hassanein and Silvestre (2013) with design rules.

4 FINITE ELEMENT MODEL

4.1 Validation

A finite element analysis is made in ANSYS using SHELL181 elements (Dekeersmaeker & Vanaerschot 2015). The model is based on experiments (Wang et al. 2014) introducing global and local geometrical imperfections, residual stresses and measured stress-strain behaviour. For the global geometrical imperfection the shape of the first eigenmode in the test set-up is used. This shape is a combination of the weak axis bending mode and a small rotation in the centre of the beam. The scale of this eigenmode is measured in the paper for every tested beam. Because stainless steel I section beams are always welded, residual stresses can have an important influence. The different material and thermal properties of stainless steel will induce a difference in shape and amplitude between carbon steel and stainless steel but also between different stainless steel families. Using the sectioning method, a residual stress measurement was conducted together with the experiments on one specimen with the same dimensions and welding procedure. A model is proposed by Wang et al. (2014), however another model Yuan et al. (2014) is chosen which is based on 10 I section stainless steel beams. This model represents all measurements accurate. Local imperfections were not measured and thus a model based on half sine waves is applied (Rossi & Li 2013).

The finite element models give a very good approximation of the ultimate load of the experiments (Table 2). However, the stiffness in the simulation is for all six experiment too high as can be seen in Figure 5. This could be a consequence of the material properties, which are based on tensile tests, despite the difference in compressive and tensile behaviour.

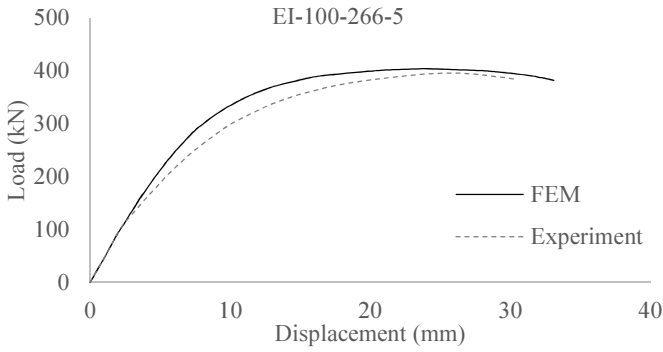


Figure 5. Comparison of experiment and FEM for load and vertical displacement at mid-span.

Table 2. Comparison of ultimate loads between the experiments and the corresponding FEM.

| Specimen | P_{exp} kN | P_{FEM} kN | P_{FEM}/P_{exp} - |
|----------|-----------------|-----------------|------------------------|
| EI-1 | 184.17 | 192.82 | 1.047 |
| EI-2 | 236.54 | 227.71 | 0.963 |
| EI-3 | 262.92 | 261.54 | 0.995 |
| EI-4 | 333.92 | 356.16 | 1.067 |
| EI-5 | 397.04 | 403.38 | 1.016 |
| EI-6 | 442.68 | 453.77 | 1.025 |
| | | AVG | 1.019 |
| | | COV | 0.036 |

4.2 Sensitivity analysis

On this model, a sensitivity analysis has been performed including the global imperfection shape and amplitude, residual stress shape and amplitude, modelling of the welds and the presence of local imperfections.

The global imperfection shape has been studied using the first eigenmode, a half-sine wave or a half sine wave with a small rotation in the middle. It can be seen that the global imperfections which include a rotation have a slightly lower ultimate load. However, the difference between the models is only 2 % and the influence on the stiffness is negligible. The change of amplitude has a far bigger significance with a difference of multiple percentages on the ultimate load but almost no effect on the stiffness. Measured global imperfection amplitudes if possible, and $L_{cr}/1000$ if not, is recommended. The buckling curves of EN 1993-1-1 are based on numerical studies with $L_{cr}/1000$ which corresponds with 80 %, as recommended in EN 1993-1-5, of the fabrication tolerance.

The shape of the residual stress distribution showed to have negligible effects. The peak tensile stress showed no difference on the ultimate load but it had a clear influence on the stiffness. However the peak tensile stress was measured (Wang et al. 2014) and confirmed by the applied model (Yuan et al. 2014), and hence the undue stiff behaviour of the model is not a result of the residual stresses.

The welds in this model were modelled using the overlap area of the shell elements and an extra beam element on both sides. The total area of the beam elements and the overlap corresponds to the area of the

welds. However, the sensitivity analysis shows that the influence of the beam elements on the ultimate load is negligible.

Local imperfections show to have a very small impact on the lateral torsional buckling behaviour and will be neglected in this paper.

4.3 Pure bending

To make a good assessment of the design rules, the basic case of pure bending with end fork conditions should be applied. For the cross-sections, dimensions are based on hot-rolled profiles: IPE 100, 600; HEA 100, 600, 1000 and HEM 100, 600, 1000. For these sections ten lengths are chosen which correspond to slenderness's between 0.2 and 1.6. Because hot-rolled stainless steel profiles are not available, welds are calculated for the ultimate shear strength $V_{pl,Rd}$. In the sensitivity analysis, it is shown that the influence of the welds is negligible. Therefore only the overlap between the web and flange is used. However for some profiles, this overlap is bigger than the area of the welds. Therefore further research and refinement concerning the modelling of the welds should be done in future works.

The boundary conditions of the model are end fork conditions which allow warping of the end section. To achieve this behaviour without convergence problems or local plastification, constraint equations are used. The middle node of the web is used as master node for the other nodes of the web. The flanges behave in a comparable way where the nodes follow the rotation of the master node (middle node) of the flange. This enables a rotation of the web around the strong axis and of the flanges around the weak axis. The flanges and web can therefore rotate apart from each other but they have to stay straight themselves. The symmetry of the sections, load case and failure mode permit to model only half the beam with a fork conditions at one end and symmetry boundary conditions which allow for in plane translations at the other end.

As a material, lean duplex is chosen because of its high strength combined with good corrosion resistance. The chosen mechanical properties, Table 3, correspond with hot rolled plates in EN 1.4062 or EN 1.4162. The used material model is a modified Ramberg-Osgood model as recommended in annex C of EN 1993-1-4 and shown in equations 9-10 with the modifications made by Arrayago et al. (2015).

For $\sigma \leq f_y$:

$$\varepsilon = \frac{\sigma}{E} + 0.002 \left(\frac{\sigma}{f_y} \right)^n \quad (9)$$

And for $f_y < \sigma \leq f_u$:

$$\varepsilon = 0.002 + \frac{f_y}{E} + \frac{\sigma - f_y}{E_y} + \varepsilon_u \left(\frac{\sigma - f_y}{f_u - f_y} \right)^m \quad (10)$$

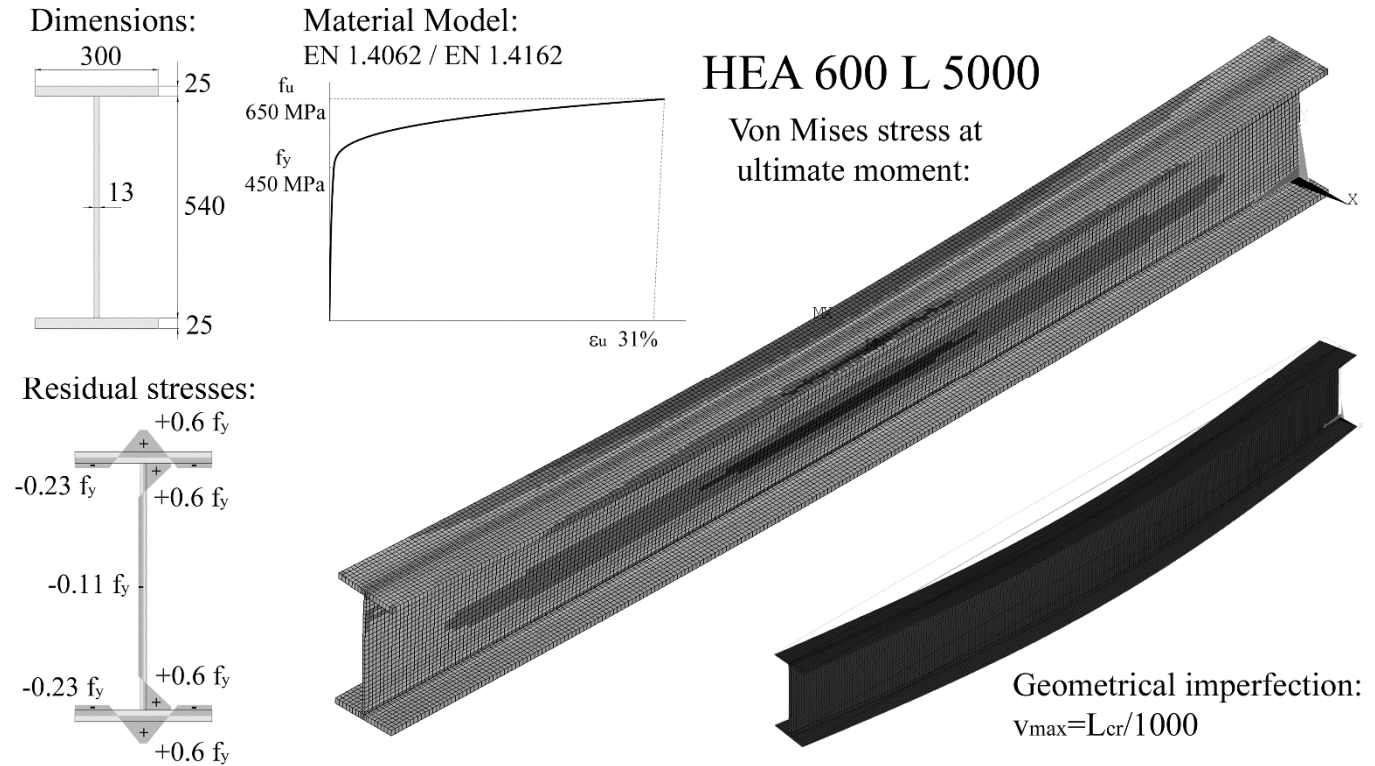


Figure 6. Pure bending finite element model HEA 600 with length 5000: Dimensions, material, imperfection and results

Table 3. Mechanical material properties for duplex EN 1.4062 and 1.4162.

| Material | EN 1.4062 / EN 1.4162 | |
|--------------|-----------------------|-------------------|
| Family | (Lean) duplex | |
| f_y | 450 | N/mm ² |
| E | 200000 | N/mm ² |
| f_u | 650 | N/mm ² |
| n | 8 | |
| m | 2.94 | |
| ϵ_u | 0.31 | |
| E_v | 24658 | N/mm ² |

Geometrical imperfections were introduced using the shape of the first eigenmode. In contrast to the experimental set-up, where this shape was a combination of the weak axis bending mode and a rotation in mid span, the fork end conditions give a first eigenmode which is purely the weak axis bending mode. However, the few very short beams have a first eigenmode which included a small distortion of the web. Further investigation will be done on the influence of the various eigenmode shapes on the lateral torsional buckling behaviour. The imperfection amplitude is rescaled to $L/1000$ for the middle node of the beam, both in length as in height. Residual stresses are introduced using both amplitude and shape of Yuan et al. (2014). A graphical summary of the used model can be found in Figure 6 which contains the Von Mises stresses at the ultimate moment.

Convergence problems arose for the HEM 100 sections with slenderness's higher than 1. These problems couldn't be solved in the frame of this paper. However, sufficient results are available to assess the lateral torsional buckling behaviour of stainless steel beams.

HEA 600 L 5000

Von Mises stress at ultimate moment:

Geometrical imperfection:
 $V_{max} = L_{cr}/1000$

5 ASSESMENT DESIGN RULES

In total 72 pure bending models were calculated and compared to the EN 1993-1-4 design rules, with the current imperfection factor 0.76 and the imperfection factor 0.49 as proposed in (Hassanein & Silvestre (2013), and to the carbon steel formulation of Taras & Greiner (2010). The results of this comparison are summarized in Table 4 and Figure 7. Figure 7. Comparison of design rules with numerical results. The smaller more stocky sections with a high W_z over W_y ratio, for example HEA 100, show an undue conservatism of the current design rules with a maximum overestimation of 1.60, Figure 7. It can be seen that for this section, Table 4, both the average value as the scatter reduces without giving unsafe results for the imperfection factor 0.49 instead of 0.76 and even more for the formulation of Taras & Greiner (2010). As can be seen in Figure 7, the design rules that use 0.49 as imperfection factor show consistent unsafe results for some sections.

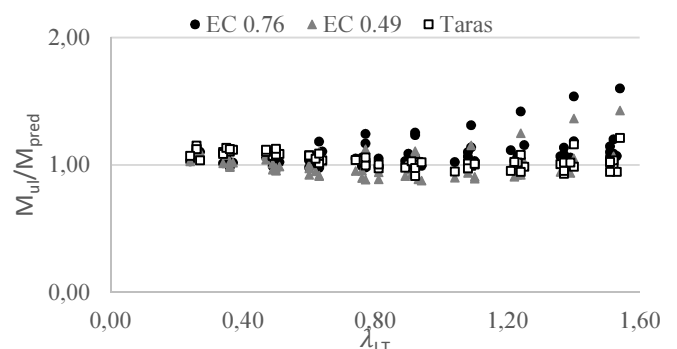


Figure 7. Comparison of design rules with numerical results.

Table 4. Comparison of design rules with the numerical results

| | EC 0.76 | | EC 0.49 | | Taras | |
|------------|---------|-------|---------|-------|-------|-------|
| | AVG | COV | AVG | COV | AVG | COV |
| <u>IPE</u> | | | | | | |
| 100 | 1.098 | 0.061 | 1.012 | 0.044 | 1.039 | 0.054 |
| 600 | 1.019 | 0.040 | 0.931 | 0.036 | 1.042 | 0.041 |
| <u>HEA</u> | | | | | | |
| 100 | 1.302 | 0.156 | 1.172 | 0.135 | 1.073 | 0.071 |
| 600 | 1.021 | 0.031 | 0.933 | 0.041 | 0.989 | 0.061 |
| 1000 | 1.074 | 0.019 | 0.994 | 0.066 | 1.043 | 0.030 |
| <u>HEM</u> | | | | | | |
| 100* | 1.161 | 0.066 | 1.100 | 0.019 | 1.063 | 0.087 |
| 600 | 1.073 | 0.047 | 0.988 | 0.044 | 1.017 | 0.069 |
| 1000 | 1.012 | 0.030 | 0.933 | 0.052 | 1.055 | 0.043 |
| ALL | 1.088 | 0.107 | 1.000 | 0.101 | 1.039 | 0.059 |

* convergence problems for slenderness's higher than 1

6 CONCLUSION

An assessment has been made for three design methods: EN 1993-1-4, with imperfection factor 0.76 and 0.49, and Taras & Greiner (2010) using both experimental and numerical results. The experimental results showed that the imperfection factor 0.49 would be the best method to design stainless steel beams. However, the numerical results show that this would lead to unsafe predictions for various sections up to 12 %. The current design rules (imperfection factor 0.76) are safe for almost all results (max 2% unsafe). However these rules show undue conservatism for stocky sections as could be noticed for carbon steel sections. The formulation of Taras & Greiner (2010) showed great promise with an average ultimate moment to predicted moment ratio of 1.039 and a small coefficient of variation of 0.059. However, improvements in imperfection factor and plateau length must be made to optimize this method for stainless steel and avoid unsafe predictions for some sections.

7 FUTURE WORK

In the next 3 years an extensive experimental program will be performed at the university of Leuven consisting of 17 tests on lateral torsional buckling and 5 ultimate moment tests on sections with a different h/b ratio and a different W_z/W_y ratio. The experimental program also includes residual stress measurements on the different sections, full 3D measurements of the initial imperfections on all specimens and various tests on the welds. Afterwards a major numerical analysis will be performed including different families and grades of stainless steel, various sections and lengths. On the basis of these results consistent design rules will be provided for the lateral torsional buckling behaviour of welded stainless steel I-beams.

8 ACKNOWLEDGEMENTS

Work by the first author was partially supported by the Research Foundation Flanders.

REFERENCES

- Arrayago, I., Real, E. & Gardner, L. 2015. Description of stress-strain curves for stainless steel alloys. *Materials & Design*, 87, 540-552.
- Baddoo, N. R. 2008. Stainless steel in construction: A review of research, applications, challenges and opportunities. *J. Constr. Steel Res.*, 64, 1199-1206.
- Burgan, B. A., Baddoo, N. R. & Gilseman, K. A. 2000. Structural design of stainless steel members comparison between Eurocode 3, Part 1.4 and test results. *Journal of Constructional Steel Research*, 54, 51-73.
- Ebel, R. & Knobloch, M. 2015. Lateral torsional buckling resistance - a comparison of analytical and numerical models. *Nordic steel construction conference*. Tampere.
- EN 1993-1-1. 2015. Eurocode 3: Design of steel structures - Part 1-1: General rules and rules for buildings. European Committee for Standardization. Brussels.
- EN 1993-1-4. 2015. Eurocode 3: Design of Steel Structures – Part 1-4: General Rules – Supplementary Rules for Stainless Steels. European Committee for Standardization. Brussels.
- Hassanein, M. F. & Silvestre, N. 2013. Flexural behavior of lean duplex stainless steel girders with slender unstiffened webs. *Journal of Constructional Steel Research*, 85, 12.
- Rossi, B. & Li, Y. 2013. Extension of the DSM to welded H profile cross-sections. *Conference proceedings: Structural Engineering, Mechanics and Computation*, 1291-1296.
- Saliba, N., Real, E. & Gardner, L. 2013. Shear design recommendations for stainless steel plate girders. *Engineering Structures*, 59, 220-228.
- Taras, A. 2010. Contribution to the development of consistent stability design rules for steel members. *Graz University of Technology*.
- Taras, A. & Greiner, R. 2010. New design curves for lateral-torsional buckling-Proposal based on a consistent derivation. *J. Constr. Steel Res.*, 66, 648-663.
- Theofanous, M. & Gardner, L. 2010. Experimental and numerical studies of lean duplex stainless steel beams. *J. Constr. Steel Res.*, 66, 816-825.
- Van Wyk, M. L., Van den Berg, G. J. & Van der Merwe, P. Lateral torsional buckling strength of doubly symmetric stainless steel beams. *International Specialty Conference on Cold-Formed Steel Structures*, 1990. 493-504.
- Wang, Y. Q., Yang, L., Gao, B., Shi, Y. J. & Yuan, H. X. 2014. Experimental Study of Lateral-torsional Buckling Behavior of Stainless Steel Welded I-section Beams. *Int. J. Steel Struct.*, 14, 411-420.
- Yang, L., Wang, Y. Q., Gao, B., Shi, Y. J. & Yuan, H. X. 2014. Two calculation methods for buckling reduction factors of stainless steel welded I-section beams. *Thin-Walled Struct.*, 83, 128-136.
- Yuan, H. X., Wang, Y. Q., Shi, Y. J. & Gardner, L. 2014. Residual stress distributions in welded stainless steel sections. *Thin-Walled Structures*, 79, 38-51.